A VISCO-PLASTIC CONSTITUTIVE MODEL FOR CYCLIC HARDENING MATERIALS AND ITS FINITE ELEMENT IMPLEMENTATION

Guozheng Kang
Department of Applied Mechanics and Engineering, Southwest Jiaotong University, Chengdu, 610031, P.R. China

Summary A visco-plastic constitutive model was extended to describe the strain-range-dependent cyclic hardening behavior and the ratcheting of SS304 stainless steel. Then the extended model was implemented into the finite element code and the simulating capability was verified by comparing with some experimental results.

Extended Summary

It has been observed that some structural materials, such as SS304 and 316 stainless steels, exhibit significant strain-range-dependent cyclic hardening. However, the existed models described only a saturated cyclic hardening of the materials, and can not simulate any non-saturation feature of cyclic hardening observed by experiments. Recently, the non-saturation feature of cyclic hardening occurred at relatively large strain ranges was successfully modeled by introducing a new constitutive description for strain-range-dependent cyclic hardening [1]. However, the previous model cannot describe the ratcheting reasonably due to the choice of Ohno-Wang model I [2]. Moreover, the implementation of an advanced constitutive model into finite element method is necessary to achieve an accurate stress-strain analysis for engineering structures. Thus, in this work, the previous model [1] is first extended to simulate the ratcheting by introducing a combined nonlinear kinematic hardening model initially developed by Abdel-Karim and Ohno [3]. Then, the extended model is implemented into finite element code, such as ABAQUS.

Constitutive model

The constitutive model to be implemented is obtained by extending the previous model [1]. The ratcheting can be described through replacing the Ohno-Wang model I [2] by Abdel-Karim-Ohno kinematic hardening rule [3], as did in [4]. Here, only the modifications to the previous models [1] [4] are emphasized.

A decomposition form of back stress $\boldsymbol{\alpha}$ is used as did in [1], i.e. $\boldsymbol{\alpha} = \sum_{k=1}^{M} r^{(k)} \mathbf{b}^{(k)}$. The critical values of dynamic recovery $r^{(k)}$ and the isotropic deformation resistance Q are variable with the evolution of cyclic hardening, which is different from that in [4]. Further, the cyclic hardening variables are decomposed as two parts: nonlinear and linear parts, $R^{NL(k)}$ and $R^{L(k)}$ respectively, and the evolution rules are adopted as $\dot{R}^{NL(k)} = C^{NL(k)}\left(R^{NLS(k)} - R^{NL(k)}\right)\dot{p}^{(k)}$ and $\dot{R}^{L(k)} = C^{L(k)}\dot{p}^{(k)}$. Where $C^{NL(k)}$, $R^{NLS(k)}$ and $C^{L(k)}$ are material constants. Thus $r^{(k)} = r_0^{(k)} + (1-\omega^{(k)})(R^{NL(k)} + R^{L(k)})$ and $Q = Q_0 + \sum_{k=1}^{M} \omega^{(k)}\left(R^{NL(k)} + R^{L(k)}\right)$, where, $r_0^{(k)}$, $\omega^{(k)}$ and Q_0 are material constants.

Finite element implementations

For the interval from step n to n+1 (i.e. $[t_n, t_{n+1}]$), using backward Euler method and following the same steps as in [4], a nonlinear scalar equation can be deduced as $\bar{Y}_{n+1} - \bar{Y}^*_{n+1} + \left(3G + \sum_{k=1}^{M} r^{(k)}_{n+1}\theta^{(k)}_{n+1}\zeta^{(k)}\right)\left\langle \frac{\bar{Y}_{n+1} - Q_{n+1}}{K} \right\rangle^n \Delta t_{n+1} = 0$. Where $r^{(k)}_{n+1}$ and Q_{n+1} are functions of Δp_{n+1}, $\bar{Y}_{n+1} = \sqrt{\tfrac{3}{2}}\left\|\mathbf{s}_{n+1} - \boldsymbol{\alpha}_{n+1}\right\|$, $\bar{Y}^*_{n+1} = \sqrt{\tfrac{3}{2}}\left\|\mathbf{s}^*_{n+1} - \sum_{k=1}^{M} r^{(k)}_{n+1}\theta^{(k)}_{n+1}\mathbf{b}^{(k)}_{n}\right\|$, and the determination of other variables can be obtained from [4]. The equation can be solved by combining successive substitution method with Newton-Raphson method for solving nonlinear equation of one variable.

Also following the same steps as in [4], a new expression of consistent tangent modulus $\mathrm{d}\Delta\boldsymbol{\sigma}_{n+1} / \mathrm{d}\Delta\boldsymbol{\varepsilon}_{n+1}$ is derived for the extended model as $\frac{\mathrm{d}\Delta\boldsymbol{\sigma}_{n+1}}{\mathrm{d}\Delta\boldsymbol{\varepsilon}_{n+1}} = \mathbf{D} - 4G^2(\mathbf{L}^{-1}_{n+1} : \mathbf{J}^0_{n+1}) : \mathbf{I}_d$, where $\mathbf{L}_{n+1} = \mathbf{I} + \mathbf{J}^0_{n+1} : (2G\mathbf{I} + \sum_{k=1}^{M}\mathbf{H}^{(k)}_{n+1}) + \sqrt{\tfrac{3}{2}}A(\mathbf{b}^0_{n+1} \otimes \mathbf{n}^0_{n+1})$, $\mathbf{H}^{(k)}_{n+1} = \left\{(1-\omega^{(k)})[C^{NL(k)}\left(R^{NLS(k)} - R^{NL(k)}_{n+1}\right) + C^{L(k)}] - r^{(k)}_{n+1}\theta^{(k)}_{n+1}\zeta^{(k)}\right\}H(f^{\#(k)}_{n+1})\mathbf{b}^{(k)}_{n+1} \otimes \mathbf{b}^{(k)}_{n+1} + \tfrac{2}{3}r^{(k)}_{n+1}\theta^{(k)}_{n+1}\zeta^{(k)}\mathbf{I}$, $\mathbf{b}'_{n+1} = \sum_{k=1}^{M}\left\{(-1)\left[1 - H\left(f^{\#(k)}_{n+1}\right)\right]r^{(k)}_{n+1}\theta^{(k)}_{n+1}\zeta^{(k)}\mu^{(k)}\mathbf{b}^{(k)}_{n+1}\right\}$, and $\mathbf{b}^0_{n+1} = \sum_{k=1}^{M}\left\{\omega^{(k)}\left[C^{NL(k)}(R^{NLS(k)} - R^{NL(k)}_{n+1}) + C^{L(k)}\right]H\left(f^{\#(k)}_{n+1}\right)\mathbf{b}^{(k)}_{n+1}\right\}$. The other items can be found in [4].

Discussion

Using the material parameters listed in Table I, the cyclic hardening behavior and ratcheting of SS304 stainless steel are simulated by the extended model and its finite element implementation. Fig. 1 shows the experimental results and the calculated ones obtained by employing a 3D 8-noded iso-parametric brick element at the strain rate of 0.2%s^{-1} under uniaxial tension. It can be seen that the calculated results for μ =0.0 and μ =0.1 are in good agreement with the experimental. If μ <0.5, its variation has little effect on the simulated stress-strain curve. From Fig. 2, it can be seen that the calculated results under symmetrical strain cycling with strain amplitude of 2%, are in good agreement with the experimental ones shown as lines in the figure and the non-saturation feature of cyclic hardening is also described.

Table I. Material constants used in numerical simulation (stress in MPa, strain mm/mm, time s)

E=1.96×10^5, v=0.33, K=82, n=13, Q_0=103;
$\zeta^{(1)}$=2242, $\zeta^{(2)}$=800, $\zeta^{(3)}$=400, $\zeta^{(4)}$=200, $\zeta^{(5)}$=133.3, $\zeta^{(6)}$=100, $\zeta^{(7)}$=66.7, $\zeta^{(8)}$=50, $\zeta^{(9)}$=40, $\zeta^{(10)}$=33.3, $\zeta^{(11)}$=28.6, $\zeta^{(12)}$=25;
r_1^0=47, r_2^0=16, r_3^0=20, r_4^0=2, r_5^0=6, r_6^0=4, r_7^0= r_8^0= r_9^0= r_{10}^0= r_{11}^0= r_{12}^0=0.001;
$R^{NLS(1)}$=13, $R^{NLS(2)}$=19, $R^{NLS(3)}$=34, $R^{NLS(4)}$=46, $R^{NLS(5)}$=35, $R^{NLS(6)}$=86, $R^{NLS(7)}$=77, $R^{NLS(8)}$=52, $R^{NLS(9)}$=48, $R^{NLS(10)}$=45, $R^{NLS(11)}$=30, $R^{NLS(12)}$=20;
$C^{NL(1)}$=$C^{NL(2)}$=$C^{NL(3)}$=25, $C^{NL(4)}$=$C^{NL(5)}$=20, $C^{NL(6)}$=$C^{NL(7)}$=5.5, $C^{NL(8)}$=$C^{NL(9)}$=7.5, $C^{NL(10)}$= $C^{NL(11)}$=$C^{NL(12)}$=10;
$C^{L(1)}$=$C^{L(2)}$=$C^{L(3)}$=$C^{L(4)}$=$C^{L(5)}$=0.0, $C^{L(6)}$=$C^{L(7)}$=14, $C^{L(8)}$=$C^{L(9)}$=29, $C^{L(10)}$=$C^{L(11)}$=$C^{L(12)}$=42;
$\omega^{(1)}$=$\omega^{(2)}$=$\omega^{(3)}$=0.15, $\omega^{(4)}$=$\omega^{(5)}$=0.45, $\omega^{(6)}$=$\omega^{(7)}$=0.55, $\omega^{(8)}$=$\omega^{(9)}$=$\omega^{(10)}$=$\omega^{(11)}$=$\omega^{(12)}$=0.70.

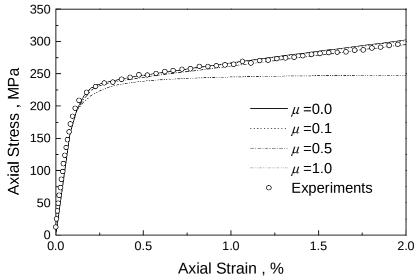

Fig. 1 Uniaxial tensile stress-strain curves

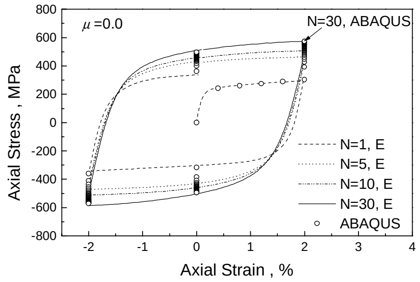

Fig. 2 Stress-strain curves for uniaxial strain cycling (μ=0.0).

An axi-symmetrical notched-bar subjected to uniaxial stress cycling with non-zero mean stress is also simulated with a 2D axi-symmetrical 4-node element mesh employed. The simulated ratcheting of the notched-bar is shown in Figs. 3 for integration points near notch-tip, and with different sub-step numbers for each half-cycle. The load condition is: $\sigma_{\max}$=200MPa; $\sigma_{\min}$=-100MPa; stress rate is 50MPas^{-1} and cyclic number is 10. It is seen that the variation of sub-step number N for each half-cycle has significant effect on the calculated ratcheting for three values of μ. The calculated result for N=3 is larger than that for N=12, and much more difference occurs as μ =0.5. It means that even the parameter μ is nearly zero, accurate simulation for the ratcheting of structure component can be only achieved by using more sub-steps (a convergent simulated result can be obtained with N=20), which is different from the conclusion obtained by [4]. This difference is also mainly caused by the introduction of $r^{(k)}$ and Q variable with cyclic hardening.

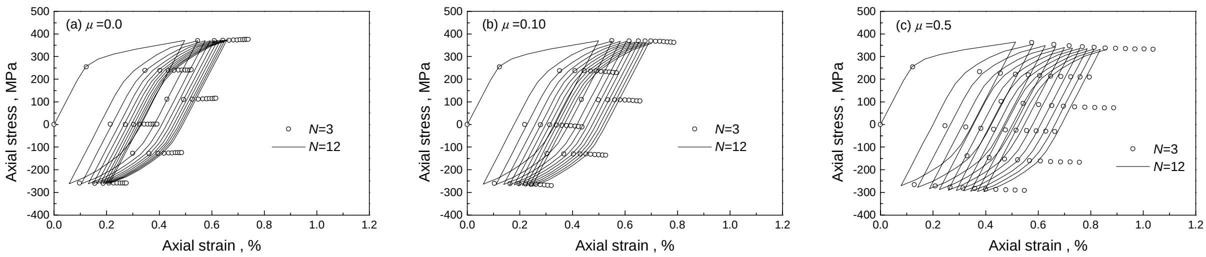

Fig. 3 Stress-strain curves of notched-bar under uniaxial stress cycling: (a) μ=0.0; (b) μ=0.1; (c) μ=0.5.

Conclusions

A visco-plastic constitutive model developed in [1] has been extended to simulate the ratcheting of cyclic hardening materials by using the Abdel-Karim-Ohno non-linear kinematic hardening rule [3], and then the extended model is implemented into a finite element code. In the numerical implementation, a new nonlinear scalar equation of implicit stress integration and a new expression of consistent tangent modulus are established. The numerical results show that an accurate simulation for the strain-controlled monotonic tension and uniaxial strain cycling can be achieved by using large strain increment with small μ, even rate-dependent plasticity is taken into account. However, under stress controlled loading, accurate simulation just can be achieved by setting stress increment small enough. Moreover, uniaxial ratcheting of structure component can be simulated reasonably by the extended model and its implementation in ABAQUS. Further, the deviatoric constitutive model used in this work will result in an almost iso-chronic behavior, and then the corresponding finite element implementation seems to be sensible to locking phenomena. This problem should be taken into account in the future modification for the extended model.

References

[1] Kang G. Z., Ohno N., Nebu A.: Constitutive modeling of strain-range-dependent cyclic hardening, *Int. J. Plasticity* 19(10): 1801-1819, 2003.

[2] Ohno N., Wang J. D.: Kinematic hardening rules with critical state of dynamic recovery. *Int. J. Plasticity* 9: 375-401, 1993.

[3] Abdel-Karim M., Ohno N.: Kinematic hardening model suitable for ratcheting with steady-state. *Int. J. Plasticity* 16:225-240, 2000.

[4] Kang G. Z.: A visco-plastic constitutive model for ratcheting of cyclically stable materials and its finite element implementation. *Mech. Mater.* 36(4): 299-312, 2004.